

Interpretation of the Gas-Phase Solvent Deuterium Kinetic Isotope Effects in the S_N2 Reaction Mechanism: Comparison of Theoretical and Experimental Results in the Reaction of Microsolvated Fluoride Ions with Methyl Halides

Gustavo E. Davico

Department of Chemistry, University of Idaho, Moscow, Idaho 83844-2343

Received: May 3, 2006; In Final Form: September 19, 2006

We carried out a comprehensive ab initio calculation and transition-state theory analysis of the solvent and secondary deuterium kinetic isotope effects in the S_N2 reactions of microsolvated fluoride ions with methyl halides. Water, methanol, and hydrogen fluoride were used as solvents, and the results are compared with recent experiments. Kinetic isotope effects were dissected into contributions from translations, rotations, and different vibration modes, and the validity of such analysis is also discussed. Excellent agreement was found for some reactions, whereas the agreement was poor for other reactions. We showed that the deviation between theory and experiments is related to the reaction kinetics; a faster reaction produced a kinetic isotope effect that was systematically larger (less inverse) than the calculated value. In addition, we also found that the magnitude of the deviation is proportional to the reaction efficiency. We rationalize the disagreement as a failure of the transition-state theory to model barrierless reactions, and we propose a very simple scheme to interpret these findings and predict the deviation between experimental and theoretical values in those reactions.

Introduction

The S_N2 reaction mechanism,¹ one of the most fundamental chemical transformations, is probably one of the best-studied mechanisms. The considerable amount of experimental and theoretical work addressing this displacement mechanism in the literature is indicative of its importance.^{2–11} The enormous amount of interest in this mechanism is justified considering that it not only plays a central role in organic chemistry but also is ubiquitous in biological systems.^{12–17}

Although early organic chemists studied the effect of the solvent in this type of reaction, it was not until more recently that this effect could be sorted out by studying these reactions using “naked” nucleophiles in the gas phase.^{3–8,18–20} In these conditions, Brauman and co-workers proposed a double-well potential-energy surface for this mechanism.⁴ Since then a wealth of experimental and theoretical data support this concept, which is widely accepted today.⁵ This is illustrated in Figure 1, where a series of potential-energy surfaces showing incrementally exothermic displacement reactions is depicted (Figure 1B). The double-well characteristic is apparent, indicating the presence of a pre- and a postreaction complex. These complexes are held together by electrostatic intermolecular forces, such as ion–dipole interactions and hydrogen bonds. In other words, the substrate “solvates” the nucleophile and the leaving group is solvated by the neutral product in the reactant side and product side complexes, respectively, which produces the double-well shape of the potential-energy surface. Under certain experimental conditions these complexes can be stabilized by removal of the excess energy. This can be accomplished, for example, using instrumentation capable of working under relatively high pressures, such as the flowing afterglow instrument, where the excess energy is collisionally transferred to the helium buffer gas. Alternatively, the complex of interest can be made by

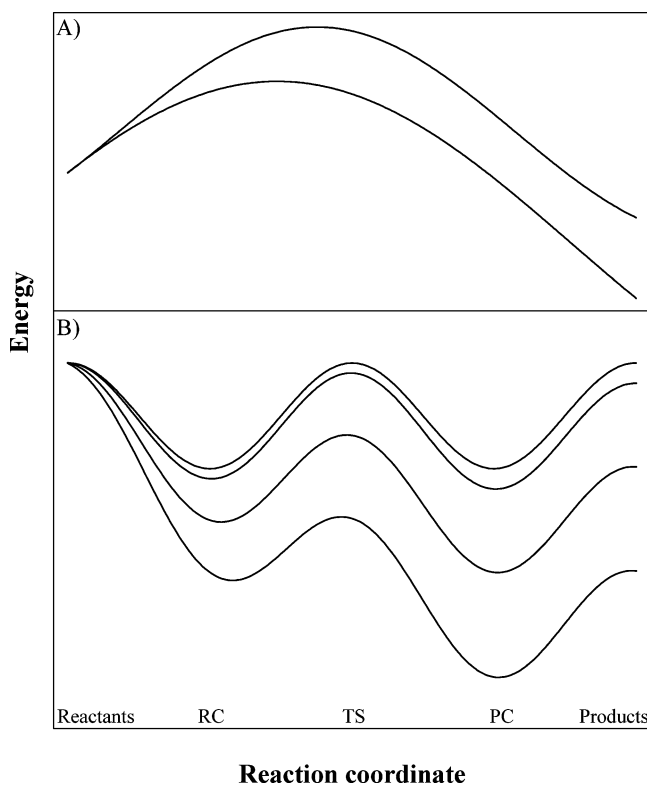


Figure 1. Illustration of the potential-energy surface for S_N2 reactions in solution (A) and the gas phase (B). In both cases the plots show reactions with different reaction exothermicities. The positions of the reaction complexes (RC), product complexes (PC), and transition states (TS) are also shown.

switching the neutral species; in other words, the naked anion is not used as the reactant but its complex with another neutral species is used instead (presumably from an endothermic reaction), which can produce the complex of interest in a

* To whom correspondence should be addressed. E-mail: davico@uidaho.edu.

reaction that is much less exothermic, increasing its lifetime and allowing it to release the excess energy by either collisions with residual gas or blackbody radiation. In solution, the nucleophile is already solvated by the solvent and these local minima in the potential-energy surface do not appear. In addition, the nucleophile needs to be desolvated to some extent before nucleophilic attack can occur, giving rise to a larger activation energy and much slower reaction rates, which have been illustrated in Figure 1A. Despite these differences, S_N2 reactions in the gas phase show similar characteristics to those carried out in solution, such as reactivity–selectivity relationships, substituents steric effects, hydrogen–deuterium isotope effects, and even competition with the E_2 mechanism, if possible at all.^{7,8,21–23}

The stabilized complex of an anion with a neutral species in the gas phase can also be considered as a microsolvated ion if the neutral is a typical solvent molecule, such as water, methanol, etc.²⁴ In addition, it is also possible to synthesize microsolvated ions with more than one solvent molecule. Pioneer work by Bohme and co-workers shows the effect of the stepwise microsolvation of nucleophiles in the S_N2 mechanism.^{25–27} They measured the rate constant for several reactions and different solvents and showed the decrease in the rate constant associated with the increased number of solvent molecules. Extrapolation of those values agrees with rates measured in bulk solution. (See Bogdanov and McMahon²⁸ for a recent review.)

The deuterium kinetic isotope effect (KIE) has also been used very successfully in studying the S_N2 reaction mechanism, in particular hydrogen–deuterium KIEs at the neutral reactant (α -deuterium KIE).^{7,8,29–33} This KIE is usually inverse; that is, the rate for the deuterium-labeled reactant is faster than the one measured for the perprotio compound ($k_H/k_D < 1$). It has been proposed earlier that this effect has its origin at the hydrogen out-of-plane bending modes that become tighter in the transition state, therefore causing a larger increase in the zero-point vibrational energy for hydrogen than for deuterium, leading to the inverse KIE.^{32–44} This interpretation of the KIEs on the S_N2 substrate has been used to predict the structure of the transition states based on the value of the experimental KIEs; a large, inverse KIE ($k_H/k_D \ll 1$) is usually associated with a tight transition state and vice versa. It has also been used in reactions taking place in confined environments, such as methyl transfer reactions catalyzed by enzymes.^{14–16,45} Several different models have been proposed to quantify the transition-state compression based on computations, commonly referred to as the transition-state tightness. Almost all of them use the nucleophile–carbon (electrophilic) bond length and the carbon–leaving group bond length, or a combination of these values, in comparison to the same bond lengths in reactants and products. All these models show some type of correlation between their particular way of measuring the transition-state compression and the calculated hydrogen–deuterium isotope effect for particular sets of S_N2 reactions.^{34,36–38,43} As Davico et al. established,³³ none of these models survive the test of a more diverse set of reactions and also demonstrated that the transition-state crowdedness is a more appropriate measure of the TS compression. The transition-state crowdedness accounts for the shape and size of the nucleophile and leaving groups in addition to the critical bond lengths and has been discussed in detail before.³³ On the basis of high-level *ab initio* computations, Truhlar and co-workers^{39–42,46,47} suggested that it is not the out-of-plane bending vibrations that are the origin of the inverse KIEs. Instead, they found that the carbon–hydrogen (deuterium) stretching vibration is the cause

as this bond becomes shorter in the transition state and the carbon atom changes its hybridization to sp^2 from sp^3 in the reactants. These authors also showed that the out-of-plane bending modes contribute with a normal (larger than 1) factor to the KIE. In addition, they also showed that the low-frequency modes, those modes that are converted from rotational and translational modes in reactants into low-frequency modes in the transition state, also contributed with a substantial inverse factor to the overall KIE. However, based on a careful analysis of individual contributions from each vibrational mode, Davico et al. later confirmed the carbon–hydrogen stretching modes as the source of the inverse KIE and argued that the contribution from this group of frequencies is rather constant and that variation observed in the KIE for different reactions is determined by the changes in the contribution from the out-of-plane bending modes,³³ in accordance with the traditional interpretation that the KIEs are indicative of the transition-state compression. In addition, they also established that the inverse contribution from the low-frequency modes reported by Truhlar et al.^{39–42,47} was an artifact of the inconsistent grouping of the different degrees of freedom. These low-frequency modes do not have their counterpart in reactants, which is equivalent to considering these frequencies as zero; however, since these frequencies are larger than zero in the transition state, the inverse KIE results (i.e., these modes are artificially considered to be tighter in the transition state). Davico et al. also showed that combining the low-frequency modes factor with the contribution from rotations and vibrations yields a slightly normal KIE (larger than 1) and that this factor is constant for similar reactions.³³

The solvent deuterium KIE in the S_N2 mechanism has been the focus of more recent attention.^{30,31,48–52} O'Hair et al. reported the first gas-phase microhydrated solvent KIE, showing that solvent KIE is very inverse, as observed in solution.³¹ Even monohydrated nucleophiles showed strongly inverse solvent KIEs. This observation contradicted the accepted theory at the moment,^{53–55} which proposed that it is the solvent structure around the transition state that is the origin of the observed inverse solvent KIE; however, with only one water molecule as solvent there is no solvent structure. Truhlar and co-workers used high-level *ab initio* calculations to show that it is one of the oxygen–hydrogen bonds in water that is the origin of the observed KIE in the $F^-(H_2O) + CH_3Cl$ reaction; this bond becomes tighter in the transition state as the hydrogen bond with the nucleophile weakens due to the transfer of charge to the leaving group as the reaction proceeds.⁵⁶ The calculated KIEs are in excellent agreement with the reported experimental values; the computed values are within the experimental error bars. However, this is not the case for all S_N2 reactions. We recently published an article reporting the experimental solvent KIEs in the S_N2 reaction of fluoride ions solvated with a variety of different molecules with methyl halides.³⁰ The results confirmed predictions from Truhlar's model; however, agreement with further theoretical values is marginal.

In this paper we are reporting theoretical results for the solvent and secondary deuterium KIEs for the reaction of fluoride ions with methyl halides. Solvents used are water, methanol, and hydrogen fluoride. These values are compared with experiments, and the origin of the difference between experiment and theory is analyzed. In addition, we also show how the difference between the calculated and experimental values for the KIE can be used in these reactions to estimate the reaction barrier. The results reported also show details of the S_N2 reaction dynamics. A complete analysis of the origin of the solvent KIE in these species is also reported.

Experimental Section

Computations were carried out using the Gaussian 98 suite of programs.⁵⁷ The 6-31++G(d,p) basis set was used, which includes not only polarization functions, but also diffuse functions to better represent loose electrons in the anions. For iodine, the LanL2DZ effective core potential^{58–60} (ECP) was used supplemented with polarization and diffuse functions (up to d functions) as proposed by Radom et al.,⁶¹ which has been used in recent articles yielding excellent results.^{62,63} In some cases, test calculations were run using the triple- ζ quality 6-311++G(d,p) basis set as well as the aug-cc-pVDZ and the aug-cc-pVTZ basis sets.^{64,65}

Geometries were optimized at the MP2 level (frozen core) followed by calculation of the force constants and harmonic vibrational frequencies of the isotopomers, which were also used to determine the zero-point vibrational energy (ZPVE, not scaled) and examine the nature of the stationary point, minimum, or transition state. Some test runs using density functional theory (DFT) were also carried out to test the performance of this method. The B3LYP correlation-exchange hybrid functional was employed for these calculations as implemented in Gaussian 98.

Further accounting for electron correlation beyond the MP2 level was not pursued since the absolute energies of the critical points in the potential-energy surfaces are not critical in this work. Instead, the difference in reaction rates for the different isotopomers is related to the accurate prediction of the vibrational frequencies, and therefore, the availability of analytical second derivatives is preferred.

The KIEs are calculated using transition-state theory (TST).⁶⁶ The use of variational transition-state theory or inclusion of tunneling has been shown to have a negligible effect on the KIEs for this type of reaction.^{39,42,47,67} The details of the calculations were reported before.³³ Briefly, the partition functions for transition states and reactants are separated into the rotational (η_{rot}), vibrational (η_{vib}), and translational (η_{trans}) components, and the factors from each of these contributions to the total KIE are calculated. In addition, the vibrational part is further partitioned into contributions from different groups of frequencies: η_{low} , frequencies that are converted from rotational and translational modes in reactants to low-frequency vibrational modes in the transition states; ($\eta_{\text{str,C-X}}$), stretching frequency between the carbon atom and the leaving group; ($\eta_{\text{str,C-H}}$), C–H stretching modes in the neutral reactant; ($\eta_{\text{ben,out}}$), out-of-plane bending modes in the neutral methyl group; ($\eta_{\text{ben,in}}$), in-plane bending modes in the neutral methyl group (scissors); ($\eta_{\text{Nu-sol}}$), stretching mode in the nucleophile–solvent interaction (the H bond); ($\eta_{\text{O-H}}$), stretching mode of the oxygen–hydrogen (H bonded) bond in the solvent ($\eta_{\text{F-H}}$ with HF as solvent); ($\eta_{\text{ben-sol}}$), bending modes in the solvent; ($\eta_{\text{str-sol}}$), stretching modes in the solvent; ($\eta_{\text{low-sol}}$), low-frequency modes in the solvent similar to η_{low} in the neutral reactant; ($\eta_{\text{ben-out-sol}}$), out-of-plane bending modes in the solvent similar to $\eta_{\text{ben,out}}$ in the neutral reactant; ($\eta_{\text{ben-in-sol}}$), scissors bending modes in the solvent similar to $\eta_{\text{ben,in}}$ in the neutral reactant; and ($\eta_{\text{str-C-H-sol}}$), C–H only stretching modes in the solvent similar to $\eta_{\text{str,C-H}}$ in the neutral reactant. Not all groups necessarily apply to every reaction; for instance, the $\eta_{\text{str-C-H-sol}}$ factors apply only to methanol and not to water or hydrogen fluoride as solvents. Each vibrational mode was carefully examined and animated and then correlated with the appropriate mode in the transition states for all reactions and every possible isotopomer in order to determine to which group it should be assigned. All calculations were carried out at 298 K.

Results and Discussion

The optimized geometries for all reactants and transition-state isotopomers are listed in the Supporting Information, including their energies and frequencies. The structures of these stationary points in the potential-energy surface are in general agreement with literature reports at different theoretical levels.^{33,42,47,56,68–70}

Results obtained at the MP2/6-31++G(d,p) and B3LYP/6-31++G(d,p) levels are shown in Table 1, including the translational, rotational, and vibrational contributions to the total KIE, for the reactions of solvated fluoride with methyl halides (Cl, Br, and I) using water (mono- and disolvated), methanol, and hydrogen fluoride as solvents. KIEs are reported for several H/D substitutions, including the neutral reactant (methyl halide), the solvent, or both. The different combinations of labeling with methanol (at the alcohol group and/or methyl group) are also included. Details of the calculations were reported before.³³ In addition, experimental values^{30,31} are also listed for comparison.

Several conclusions can be quickly drawn from Table 1. Clearly, all KIEs are inverse (<1) regardless of the location of the H/D substitution, in agreement with experiment (gas and condensed phase) and previous computations. In addition, it seems that the solvent KIEs produced from the group H bonded to the nucleophile (around 0.6) are substantially more inverse than those from the neutral reactant (around 0.8). The solvent KIEs from the methyl group in methanol show similar values (around 0.8) to those from the neutral reactant (methyl halide), which is rather surprising since the methyl group in methanol is quite far from the reaction center. The translational and rotational contributions to the KIE are normal (>1), whereas the vibrational part is quite inverse, as reported before for several S_N2 reactions.^{33,42,46,47,56} There is also indication that the MP2/6-31++G** level produces reliable KIE values. For example, our values for the reaction of $\text{F}^-(\text{H}_2\text{O})$ with methyl chloride are practically the same as those reported before at the MP2/aug-cc-pVDZ level⁵⁶ and are in excellent agreement with the experimental values, suggesting that the model is quantitatively valid. The results at the B3LYP/6-31++G** level for the same reactions do not agree with experiments. The same disagreement is observed with HF as the solvent. The origin of the disagreement seems to be in the vibrational part, suggesting that the B3LYP method has difficulties in modeling the frequencies, which is surprising; however, it has been reported that DFT methods produce poor central barriers in S_N2 reactions and presumably incorrect structures and frequencies.^{71,72} For the neutral KIE the latter theoretical model also predicts a noticeably less inverse (closer to 1) vibrational contribution and total KIE. For some of the reactions included in Table 1 the DFT values seem to agree better with experiments; however, this situation is rather fortuitous as discussed below.

Usually a normal KIE is associated with an isotopically active normal mode becoming weaker as a reaction proceeds from the reactants to the transition state and, conversely, an inverse KIE is linked to a mode becoming stronger in the transition state. In more general terms, an inverse KIE is observed when the zero-point energy is larger in the transition state than in the reactants, yielding a larger zero-point energy difference between the isotopes in the transition state that increases the activation barrier for the light isotope, as shown in Figure 2. Therefore, it is not surprising that the vibrational contributions to the total KIE in Table 1 are the only inverse contributions. In addition, Truhlar and co-workers showed that the translational and particularly rotational contributions are large and normal, which could potentially outweigh the inverse vibrational part.^{47,56}

TABLE 1: Factor Analysis of the Kinetic Isotope Effects in the Solvated S_N2 Reactions

reaction	η_{trans}	kinetic isotope effect ($k_{\text{H}}/k_{\text{D}}$) ^a				experimental ^b
		η_{rot}	η_{vib}	η_{total}		
F ⁻ (H ₂ O) + CH ₃ Cl/CD ₃ Cl	1.04 (1.04)	1.63 (1.63)	0.51 (0.55)	0.86 (0.92)	0.85 ± 0.03	
F ⁻ (H ₂ O) + CH ₃ Br/CD ₃ Br	1.01 (1.01)	1.61 (1.62)	0.52 (0.55)	0.84 (0.90)	0.92 ± 0.02	
F ⁻ (H ₂ O) + CH ₃ I/CD ₃ I	1.01 (1.01)	1.64 (1.64)	0.51 (0.57)	0.84 (0.94)	0.92 ± 0.05	
F ⁻ (D ₂ O) + CH ₃ Cl/CD ₃ Cl	1.04	1.63	0.51	0.86	0.86 ± 0.03	
F ⁻ (D ₂ O) + CH ₃ Br/CD ₃ Br	1.01	1.62	0.52	0.84	0.93 ± 0.02	
F ⁻ (D ₂ O) + CH ₃ I/CD ₃ I	1.01	1.65	0.51	0.84	0.95 ± 0.05	
F ⁻ (H ₂ O/D ₂ O) + CH ₃ Cl	1.05 (1.05)	1.34 (1.35)	0.46 (0.45)	0.65 (0.63)	0.65± 0.03	
F ⁻ (H ₂ O/D ₂ O) + CH ₃ Br	1.06 (1.06)	1.36 (1.36)	0.45 (0.44)	0.65 (0.63)	0.83± 0.02	
F ⁻ (H ₂ O/D ₂ O) + CH ₃ I	1.07 (1.07)	1.34 (1.34)	0.47 (0.46)	0.67 (0.66)	0.89± 0.05	
F ⁻ (H ₂ O/D ₂ O) + CD ₃ Cl	1.05	1.35	0.46	0.65	0.65± 0.02	
F ⁻ (H ₂ O/D ₂ O) + CD ₃ Br	1.06	1.36	0.45	0.65	0.84± 0.02	
F ⁻ (H ₂ O/D ₂ O) + CD ₃ I	1.07	1.34	0.47	0.67	0.91± 0.05	
F ⁻ (H ₂ O) ₂ /(D ₂ O) ₂ + CH ₃ I	1.08	1.03	0.59	0.66	0.7 ± 0.15	
F ⁻ (CH ₃ OH) + CH ₃ Br/CD ₃ Br	1.02	1.70	0.49	0.85	0.86 ± 0.02	
F ⁻ (CH ₃ OD) + CH ₃ Br/CD ₃ Br	1.02	1.70	0.49	0.85	0.91 ± 0.02	
F ⁻ (CD ₃ OH) + CH ₃ Br/CD ₃ Br	1.02	1.71	0.49	0.85	0.92 ± 0.04	
F ⁻ (CD ₃ OD) + CH ₃ Br/CD ₃ Br	1.02	1.71	0.49	0.85	0.90 ± 0.01	
F ⁻ (CH ₃ OH) + CH ₃ I/CD ₃ I	1.01	1.70	0.49	0.84	0.90 ± 0.02	
F ⁻ (CH ₃ OD) + CH ₃ I/CD ₃ I	1.01	1.70	0.49	0.84	0.90 ± 0.02	
F ⁻ (CD ₃ OH) + CH ₃ I/CD ₃ I	1.01	1.71	0.49	0.84	0.92 ± 0.02	
F ⁻ (CD ₃ OD) + CH ₃ I/CD ₃ I	1.01	1.71	0.49	0.84	0.94 ± 0.02	
F ⁻ (CH ₃ OH/CH ₃ OD) + CH ₃ Br	1.02	0.99	0.64	0.64	0.73 ± 0.02	
F ⁻ (CH ₃ OH/CD ₃ OH) + CH ₃ Br	1.06	1.12	0.74	0.88	0.83 ± 0.03	
F ⁻ (CD ₃ OH/CD ₃ OD) + CH ₃ Br	1.02	0.99	0.64	0.64	0.71 ± 0.02	
F ⁻ (CD ₃ OH/CD ₃ OD) + CD ₃ Br	1.02	0.99	0.64	0.64	0.69 ± 0.03	
F ⁻ (CH ₃ OH/CD ₃ OD) + CH ₃ Br	1.08	1.11	0.47	0.56	0.59 ± 0.02	
F ⁻ (CH ₃ OH/CD ₃ OH) + CD ₃ Br	1.06	1.12	0.74	0.88	0.89 ± 0.03	
F ⁻ (CH ₃ OD/CD ₃ OD) + CD ₃ Br	1.06	1.12	0.74	0.88	0.80 ± 0.01	
F ⁻ (CH ₃ OD/CD ₃ OD) + CH ₃ Br	1.06	1.12	0.74	0.88	0.81 ± 0.01	
F ⁻ (CH ₃ OH/CH ₃ OD) + CH ₃ I	1.02	0.99	0.64	0.65	0.88 ± 0.02	
F ⁻ (CH ₃ OH/CD ₃ OH) + CH ₃ I	1.07	1.12	0.73	0.87	0.90 ± 0.02	
F ⁻ (CD ₃ OH/CD ₃ OD) + CH ₃ I	1.02	0.99	0.64	0.65	0.84 ± 0.02	
F ⁻ (CD ₃ OH/CD ₃ OD) + CD ₃ I	1.02	0.99	0.64	0.65	0.86 ± 0.02	
F ⁻ (CH ₃ OH/CD ₃ OD) + CH ₃ I	1.09	1.11	0.47	0.57	0.76 ± 0.02	
F ⁻ (CH ₃ OH/CD ₃ OH) + CD ₃ I	1.07	1.12	0.73	0.87	0.93 ± 0.02	
F ⁻ (CH ₃ OD/CD ₃ OD) + CD ₃ I	1.07	1.12	0.73	0.87	0.90 ± 0.02	
F ⁻ (CH ₃ OD/CD ₃ OD) + CH ₃ I	1.06	1.12	0.73	0.87	0.87 ± 0.02	
F ⁻ (HF) + CH ₃ I/CD ₃ I	1.01 (1.01)	1.65 (1.66)	0.48 (0.53)	0.80 (0.89)	0.78 ± 0.03	
F ⁻ (HF/DF) + CH ₃ I	1.03 (1.03)	0.98 (0.98)	0.56 (0.61)	0.56 (0.61)	0.59 ± 0.01	

^a Computed at the MP2/6-31++G(d,p) level and using conventional transition-state theory. Values in parentheses are at the B3LYP/6-31++G(d,p) level. The LANL2DZ ECP, supplemented with diffuse and polarization functions, is used for iodine; see text for details. See the Experimental Section for a definition of the different factors. ^b Taken from refs 30 and 31.

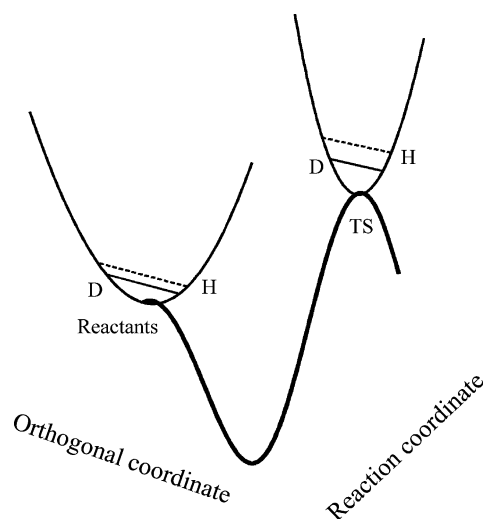


Figure 2. Schematic of a potential-energy surface showing a bound coordinate that becomes more strongly bound in the transition state, producing an inverse H/D KIE.

However, it was later demonstrated³³ that this is an artifact arising from the artificial separation of the rotational, translational, and vibrational degrees of freedom since in a bimolecular

reaction some translations and rotations in reactants are converted into vibrations in the transition state. Therefore, a balance of equivalent degrees of freedom between reactants and transition states is not established, yielding misleading values. For instance, the new bound vibrational modes in the transition state that correlate with rotations and translations in reactants, which are calculated as zero, would produce an inverse KIE, as predicted using Figure 2. Therefore, analysis of the rotational and translational contributions is not adequate, and the product of these two factors and the corresponding new frequency group (usually low-frequency modes) should be used instead. This issue has been discussed already in detail for unsolvated S_N2 reactions.³³

A more detailed analysis of the contributions from different frequency groups to the vibrational component of the total KIE is presented in Tables 2, 3, and 4 for water, methanol, and hydrogen fluoride as solvents, respectively (see the Experimental Section for the group definitions). In addition, the products of the rotational, translational, and the low vibrational modes are also shown in the last column of Tables 2–4. The products of these three factors show values of 1.00 and 1.10 for the solvent and neutral KIE, respectively, regardless of the nucleophile,³³ solvent, or neutral reactant considered. Therefore, this consistent, correlated group of degrees of freedom does not contribute or

TABLE 2: Factor Analysis of the Vibrational Component of the Kinetic Isotope Effects in the Reaction of $F^-(H_2O) + CH_3X^a$

reaction	η_{low}	$\eta_{str,C-X}$	$\eta_{ben,out}$	$\eta_{ben,in}$	$\eta_{str,C-H}$	$\eta_{ben,solv}$	$\eta_{Str-solv}$	$\eta_{Nu-solv}$	η_{O-H}	$\eta_{vib,total}$	$\eta_{low}\eta_{trans}\eta_{rot}$
$F^-(H_2O) + CH_3Cl/CD_3Cl$	0.66 (0.65)	1.05 (1.05)	0.87 (0.94)	1.19 (1.20)	0.72 (0.72)	1.00 (1.01)	1.00 (0.97)	0.99 (0.99)	1.00 (1.00)	0.51 (0.55)	1.11
$F^-(H_2O) + CH_3Br/CD_3Br$	0.67 (0.66)	1.04 (1.04)	0.85 (0.91)	1.18 (1.19)	0.75 (0.74)	1.00 (1.01)	1.00 (1.00)	0.99 (0.99)	1.00 (1.00)	0.52 (0.55)	1.09
$F^-(H_2O) + CH_3I/CD_3I$	0.66 (0.65)	1.06 (1.06)	0.86 (0.95)	1.15 (1.16)	0.75 (0.76)	1.01 (1.00)	1.00 (1.00)	0.99 (0.99)	1.00 (1.00)	0.51 (0.57)	1.09
$F^-(H_2O/D_2O) + CH_3Cl$	0.70 (0.74)	0.99 (0.94)	0.99 (1.00)	1.00 (1.00)	1.00 (1.00)	1.26 (1.23)	0.99 (0.99)	1.03 (1.03)	0.52 (0.52)	0.46 (0.45)	0.99
$F^-(H_2O/D_2O) + CH_3Br$	0.68 (0.69)	0.99 (0.99)	1.00 (0.99)	1.00 (1.00)	1.00 (1.00)	1.24 (1.22)	0.99 (0.99)	1.03 (1.02)	0.54 (0.53)	0.45 (0.44)	0.98
$F^-(H_2O/D_2O) + CH_3I$	0.69 (0.70)	1.00 (0.99)	0.99 (1.00)	1.00 (1.00)	1.00 (1.00)	1.24 (1.18)	0.99 (0.99)	1.02 (1.02)	0.55 (0.56)	0.47 (0.46)	0.99
$F^-(H_2O)_2/(D_2O)_2 + CH_3I^b$	0.92	0.99	1.00	1.00	1.00	1.36	1.04		0.46	0.59	1.02

^a Computed at the MP2/6-31++G(d,p) level and using conventional transition-state theory. Values in parentheses are at the B3LYP/6-31++G(d,p) level. The LANL2DZ ECP, supplemented with diffuse and polarization functions, is used for iodine; see text for details. See the Experimental Section for a definition of the different factors. ^b A complete identification and classification of the different modes in this reaction is very difficult since some modes that would be part of different factors are highly coupled. Therefore, all solvent internal modes were included in the $\eta_{Str-solv}$ and $\eta_{ben-solv}$ factors, with the exception of the O–H stretching mode in the solvent.

TABLE 3: Factor Analysis of the Vibrational Component of the Kinetic Isotope Effects in the Reaction of $F^-(CH_3OH) + CH_3X^a$

reaction	η_{low}	$\eta_{str,C-X}$	$\eta_{ben,out}$	$\eta_{ben,in}$	$\eta_{str,C-H}$	$\eta_{ben,sol}$	$\eta_{str-sol}$	$\eta_{low,sol}$	$\eta_{ben,out-sol}$	$\eta_{ben,in-sol}$	$\eta_{str,C-H-sol}$	η_{Nu-sol}	η_{O-H}	$\eta_{vib,total}$	$\eta_{low}\eta_{trans}\eta_{rot}$
$F^-(CH_3OH) + CH_3Br/CD_3Br$	0.64	1.05	0.85	1.18	0.75	0.99	1.00	0.99	1.00	1.00	1.00	0.99	1.00	0.49	1.11
$F^-(CH_3OH) + CH_3I/CD_3I$	0.64	1.07	0.87	1.15	0.75	0.98	1.00	1.00	1.00	1.00	1.00	0.99	1.00	0.49	1.10
$F^-(CH_3OH/CH_3OD) + CH_3Br$	0.98	1.00	1.00	1.00	1.00	0.80	1.01	1.00	1.74	0.98	1.02	1.02	0.46	0.64	0.99
$F^-(CH_3OH/CD_3OH) + CH_3Br$	0.85	1.00	1.00	1.00	1.00	0.98	1.03	0.99	0.94	1.01	1.00	1.01	0.92	0.74	1.01
$F^-(CH_3OH/CH_3OD) + CH_3I$	0.98	1.00	1.01	1.00	1.00	0.75	1.01	0.99	1.73	1.03	1.03	1.02	0.47	0.64	0.99
$F^-(CH_3OH/CD_3OH) + CH_3I$	0.84	1.00	1.00	1.00	1.00	0.98	1.03	1.00	0.95	1.01	1.00	1.00	0.91	0.73	1.01

^a Computed at the MP2/6-31++G(d,p) level and using conventional transition-state theory. The LANL2DZ ECP, supplemented with diffuse and polarization functions, is used for iodine; see text for details. See the Experimental Section for a definition of the different factors.

TABLE 4: Factor Analysis of the Vibrational Component of the Kinetic Isotope Effects in the Reaction of $F^-(HF) + CH_3I^a$

reaction	η_{low}	$\eta_{str,C-X}$	$\eta_{ben,out}$	$\eta_{ben,in}$	$\eta_{str,C-H}$	$\eta_{ben,sol}$	η_{Nu-sol}	η_{F-H}	$\eta_{vib,total}$	$\eta_{low}\eta_{trans}\eta_{rot}$
$F^-(HF) + CH_3I/CD_3I$	0.65	1.06	0.84	1.15	0.75	0.99	0.99	1.00	0.48	1.08
$F^-(HF/DF) + CH_3I$	0.99 (0.99)	1.00 (1.00)	1.01 (1.01)	1.00 (1.00)	1.00 (1.00)	1.33 (1.26)	0.98 (0.98)	0.43 (0.50)	0.56 (0.61)	1.00

^a Computed at the MP2/6-31++G(d,p) level and using conventional transition-state theory. Values in parentheses are at the B3LYP/6-31++G(d,p) level. The LANL2DZ ECP, supplemented with diffuse and polarization functions, is used for iodine; see text for details. See the Experimental Section for a definition of the different factors.

contributes only slightly and in a normal way to the total KIE, in agreement with our previous results for unsolvated S_N2 reactions.³³

The neutral KIEs (from the methyl halides) show inverse contributions from the C–H stretching and out-of-plane bending modes, whereas the other groups show normal or no contribution to the vibrational KIE, in agreement with other S_N2 reactions. Usually the first term is inverse whereas the second depends strongly on the transition-state crowdedness, as defined and discussed in detail before.³³ In the reactions reported here, the solvent molecule contributes to the transition-state crowdedness yielding an inverse contribution from the out-of-plane bending modes. It is interesting to note that the origin of the disagreement at the B3LYP level is surprisingly due only to the out-of-plane bending modes. The contribution to the KIE from this group of frequencies is systematically predicted to be less inverse at this level, whereas all other frequency groups yield the same results as those obtained at the MP2 level. Similar results on group contributions for the neutral KIEs are also observed for methanol and HF as solvents (Tables 3 and 4).

As mentioned before, the solvent KIEs show markedly more inverse values than those originating from the neutral reactants. Although for monohydrated reactions most groups of frequency modes provide little or no contribution to the vibrational KIE, the values of the O–H stretching and the solvent bending modes

deviate substantially from unity. The first group shows inverse contributions, whereas the last group shows normal contributions. The O–H stretching mode is clearly the most important factor and has its origin in the O–H (H bonded) bond in water that becomes stronger in the transition state as the charge is transferred to the leaving group, which was first recognized by Truhlar⁵⁶ (see Figure 2). The inverse KIE effect caused by this mode is partially neutralized by the normal contribution from the solvent bending modes group. This group is composed of three modes that include internal rotations and bending of the $F^-(H_2O)$ moiety that becomes looser in the transition state (and therefore the normal contribution) as the interaction between the nucleophile and water becomes less important due to the charge being transferred to the leaving group.

Similar results are found in the reaction involving the dihydrated fluoride ion, showing a more inverse KIE value from the O–H stretching mode, which in this case is surpassed by an even larger increase from the solvent bending modes group.

For the reactions with methanol as solvent a similar trend is observed with only a few groups contributing values that differ substantially from unity (Table 3). As expected, the O–H stretching mode group is considerably inverse, even more than in the case of water, when the alcohol group is labeled; however, the value is close to unity when the methyl group is labeled instead. The other two active groups are the solvent internal

bending modes and the solvent methyl group out-of-plane bending modes, which include the umbrella mode. These groups show inverse and normal contributions, respectively, when the alcohol group is labeled, whereas their contributions are very close to unity when the methyl group is labeled instead. Although the solvent bending modes group in methanol contains the same number of analogous modes as in water, the contribution from this group is inverse in the former but normal in the latter upon deuteration of the $-OH$ group. Closer examination of these modes shows couplings between some of these modes with others arranged in the out-of-plane and in-plane bending modes of the methyl group in methanol. Therefore, there might be some misleading deviations from unity in these groups. Overall, the contribution is normal when considered together. Deuteration of the methyl group in methanol shifts the frequencies, and coupling is no longer observed. In this case an inverse contribution is observed, which is particularly important from the solvent out-of-plane bending modes group, similar to the contributions from the same group of modes observed upon deuteration of the methyl group in the methyl halides, although not as pronounced. These results are consistent with the tightening of these modes as the solvent regains a structure that is more similar to a free solvent molecule in the transition state. The grouping of vibrational modes and analyses becomes very difficult with methanol as solvent due to coupling between some modes; however, the other H/D labeling combinations, which are all shown in Table 1, yield similar results and are not included in Table 3.

The reactions involving HF as solvent are very interesting since they provide an example of a relatively higher acidic solvent; an even more acidic solvent will necessarily switch the effective nucleophile to the solvent conjugated base. The results for HF are not much different from those for water, showing a very inverse contribution from the hydrogen-bonded H–F bond, which is partially offset by a normal solvent bending mode (Table 4). Again the B3LYP method yields different values from MP2, although in this case the deviations from unity in the solvent bending mode and the H–F stretching mode partially cancel each other, yielding a total vibrational contribution that is slightly larger than the value obtained at the MP2 level.

A detailed comparison between the calculated and experimental values in Table 1 shows that although there is excellent agreement in several entries, the agreement is poor in some other cases. For instance, with water as solvent there is excellent agreement in the reaction with methyl chloride in both solvent and neutral KIEs; however, the values are quite different for methyl bromide and even worse for methyl iodide. It is interesting to note that the calculated values are consistently more inverse than the experimental ones. The agreement between experiment and theory is excellent in both reactions involving HF as solvent. A similar situation is also found with methanol as solvent with the exception of the solvent methyl group KIEs, which show deviations in the opposite direction, i.e., calculated values that are less inverse than experimental values. The source of the disagreement could be attributed in principle to an incomplete basis set or an inadequate theoretical model; therefore, we ran some test calculations using more complete basis sets to check for convergence. The results indicate that the deviations in the solvent methyl group KIEs are closer to the experimental values when using a more complete basis set. For instance, we calculated 0.85 as the KIE for the reaction $F^-(CH_3OD/CD_3OD)$ with methyl bromide at the MP2/6-311++G(d,p) level, closer to the experimental value

of 0.81 (see Table 1), suggesting that in these cases the disagreement between experiment and theory can be solved using a more complete basis set (or presumably a method that accounts for more dynamic electron correlation).

For those cases in which there is agreement, use of a more complete basis set did not usually yield different results, suggesting convergence was achieved. For instance, KIE values of 0.84 and 0.65 were obtained for $F^-(H_2O)$ with CH_3Cl/CD_3Cl and $F^-(H_2O/D_2O)$ with CH_3Cl at the MP2/aug-cc-pVDZ level, respectively, in agreement with earlier reports⁵⁶ and the values in Table 1. However, for those reactions in which the calculated and experimental values disagree, we generally found that a more complete basis set either agreed with the lower level value, the values converged, or they were even more inverse, i.e., increased the difference between theory and experiment. For example, a value of 0.59 was obtained for the KIE in the reaction of $F^-(CH_3OH/CH_3OD)$ with CH_3Br at the MP2/6-311++G(d,p) level, in disagreement with the 0.73 ± 0.02 value obtained experimentally and more inverse than the 0.64 value obtained at the MP2/6-31++G(d,p) level (Table 1); therefore, going from a double- to a triple- ζ basis set increased the disagreement with experimental results. Hu and Truhlar reported a similar situation for the S_N2 reactions of Cl^- and Br^- with methyl halides,³⁹ which prompted an experimental reevaluation of the KIEs, reinforcing the disagreement between theory and experiment in these reactions.²⁹ In addition, it has been shown that the use of other theoretical models, including variational TST and inclusion of tunneling, yields essentially the same results.^{39,47} Therefore, there must be a different explanation for the disagreements.

More careful analysis of the data shown in Table 1 suggests that the disagreement between calculated and experimental KIEs might be dependent on the reaction kinetics. Computing the KIEs is considerably more accurate than the calculation of absolute rate constants, since frequencies and geometries are predicted with reasonable accuracy by the models used in this report, while that is certainly not the case for their energies, especially for the transition states. To establish the relative accuracy of our theoretical model we plotted the free energy of activation⁵⁷ for all reactions shown in Table 1, including the unsolvated S_N2 reactions, versus the reaction efficiency. The reaction efficiency is a measure of the fraction of collisions that lead to products and is computed as the ratio between the experimental rate constant^{30,31} and the collisional rate constant.⁷³ The plot, shown in Figure 3, clearly shows good correlation between the calculated free energy of activation and the reaction efficiency, suggesting that, as can be anticipated, the reaction efficiency provides an indication of the reaction barrier and the theoretical model used is adequate. In addition, the correlation is surprisingly good considering that the basis set used for iodine (actually a supplemented ECP, see Experimental Section) is different from the one used for the other halogens; in fact, better correlation is observed if the reactions involving iodine are considered separately. We should emphasize that only the correlation is important at this point (at a particular theoretical level) and not the absolute values for the free energy of activation, which, as mentioned below, is expected to decrease as better theoretical models are used. For instance, the free energy of activation is predicted to be positive for all solvated reactions; however, it might become negative for some reactions using a more complete model as better accounting for electron correlation would generally stabilize the transition states more than the reactants. Indeed, our calculations predict a small positive activation energy for the reaction of $F^-(H_2O)$ with

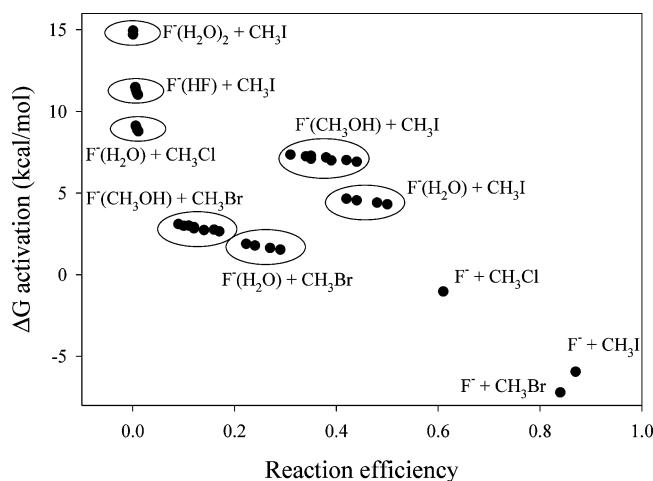


Figure 3. Plot of the free energy of activation calculated at the MP2/6-31++G(d,p) level (supplemented ECP for iodine, see Experimental Section) versus the reaction efficiency ($k_{\text{exp}}/k_{\text{col}}$, k_{exp} from refs 30 and 31, whereas k_{col} is calculated according to ref 73) for the isotopomers shown in Table 1.

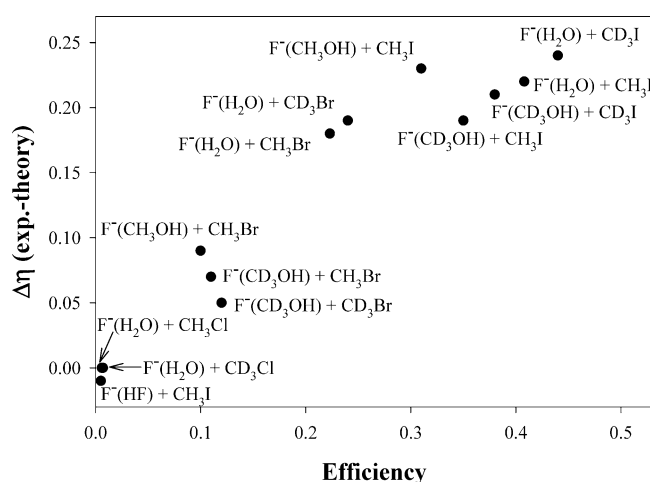


Figure 4. Plot of the difference between the experimental and the calculated (MP2/6-31++G(d,p) level and supplemented ECP for iodine, see Experimental Section) KIEs for the solvent $-\text{OH}(\text{FH})$ versus the reaction efficiency ($k_{\text{exp}}/k_{\text{col}}$, k_{exp} from refs 30 and 31, whereas k_{col} is calculated according to ref 73).

CH_3Br , whereas experimental results⁴⁸ show a negative temperature dependence for the rate constant consistent with a negative activation barrier; however, as discussed above, the absolute values for the activation energies are not critical in this discussion.

Taking the reaction efficiency as a measure of reactivity, we found that the reactivity is indeed related to the difference between the calculated and experimental KIEs, i.e., the faster the reaction the larger the disagreement. The correlation between these quantities is shown in Figures 4, 5, and 6 for the H/D KIEs at the solvent $-\text{OH}(\text{HF})$, solvent methyl group, and neutral reactant, respectively. The KIEs associated with the $-\text{OH}(\text{HF})$ groups (the hydrogen atom H bonded to the nucleophile) are more pronounced and so are the deviations observed from the calculated values. The deviations are around zero for slow reactions with small efficiencies and relatively larger activation barriers and around 0.25 for fast reactions with efficiencies approaching 0.5. In general, this observation is qualitatively reasonable, as a faster reaction would be less selective. However, it points out the failure of the TST to predict the gradual change in KIEs as the reaction becomes faster and the reaction barrier decreases.

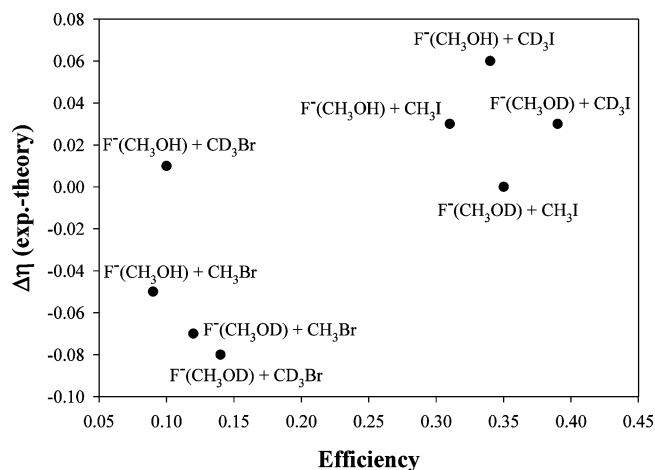


Figure 5. Plot of the difference between the experimental and the calculated (MP2/6-31++G(d,p) level and supplemented ECP for iodine, see Experimental Section) KIEs for the methyl group in methanol versus the reaction efficiency ($k_{\text{exp}}/k_{\text{col}}$, k_{exp} from refs 30 and 31, whereas k_{col} is calculated according to ref 73).

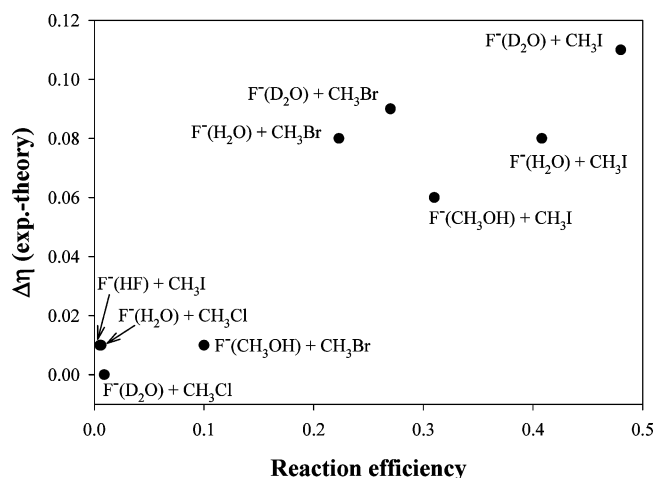


Figure 6. Plot of the difference between the experimental and the calculated (MP2/6-31++G(d,p) level and supplemented ECP for iodine, see Experimental Section) KIEs for the neutral substrate versus the reaction efficiency ($k_{\text{exp}}/k_{\text{col}}$, k_{exp} from refs 30 and 31, whereas k_{col} is calculated according to ref 73).

A similar trend is observed with the KIEs for the methyl group in methanol when it is used as the solvent, although in this case the KIE values are smaller and so are the deviations, yielding a plot that seems more scattered. However, we think that is because the deviations are becoming of the same magnitude as the error bars, since the errors associated with only the experimental KIEs are in the order of 0.02–0.03. In addition, this set of KIE difference values shows substantial negative deviation values for reactions with small efficiencies, that is, calculated KIEs that are larger (less inverse) than experimental KIEs, which is related to the inadequacy of the theoretical model to predict accurately these low-order KIEs and corrected using a more complete basis set, as discussed above. In any case, this issue is of relative importance since it is the trend in which we are interested and use of a different model would yield different values for $\Delta\eta$ but a similar trend. Finally, an intermediate behavior is observed in Figure 6 for the neutral KIEs, with KIEs and $\Delta\eta$ values that are larger and smaller than those shown in Figures 4 and 5, respectively, and show less scattering. However, the same trend is clear: the faster the reaction, the larger the difference between calculated and experimental KIEs.

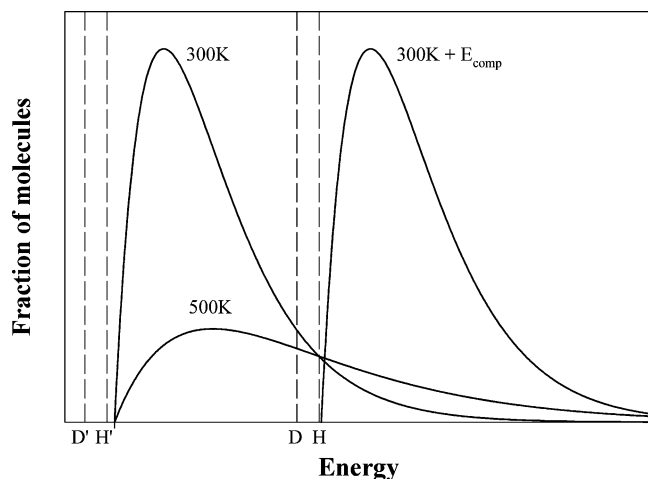


Figure 7. Plot of the Boltzmann distribution at 300 and 500 K, showing the larger KIE expected at the lower temperature (H and D) as a larger fraction of molecules can surmount the lower barrier for deuterium. Also shown is the shift of the distribution produced by the complexation energy (E_{comp}) as proposed in refs 21 and 22 (note that this distribution is now referenced to the complex energy and not to reactants). In addition, similar barriers for a reaction with negative activation energy are shown (D' and H').

Two hypothetically extreme situations can be anticipated in these reactions from a kinetic perspective. On one extreme would be reactions that have positive or near zero activation energies. In these very slow reactions surmounting the transition-state structure would be the rate-limiting step. The other extreme would be very fast reactions with large negative activation barriers. For these reactions the association rate would be the rate-limiting process (Figure 1).

The TST unequivocally yields excellent results for reactions that are slow and therefore have transition states with energies that are comparable to or larger than the corresponding reactants. In these reactions crossing over the transition state is the rate-limiting step, as for reactions in solution, and most collisions do not have enough energy to cross the barrier and dissociate back to reactants. The presence of the reactant complex in the potential-energy surface (PES) might affect the reaction dynamics depending on whether the excess energy in the complex does or does not equilibrate within its lifetime. During a collision with an ideal orientation in which the reaction proceeds through the lowest energy pathway, i.e., linear, the potential energy would couple efficiently into kinetic energy along the reaction coordinate. In these collisions the complex cannot be considered thermally hot and instead shows an internal distribution of energy (with the complex energy as reference) that resembles that of reactants shifted by the complexation energy. This issue has been discussed in detail recently in the context of the selectivity observed in gas-phase reactions.^{21,22} As shown in Figure 7, the reactants would have a Boltzmann distribution of energies according to their temperature (in this case we used 300 K), and a positive reaction barrier would yield a faster reaction for deuterium, with a lower barrier, than for hydrogen (marked D and H, respectively, in Figure 7). Assuming equilibration of the complexation energy (or a large portion of it) within the complex would imply an increase in the effective temperature and a decrease in the reaction selectivity, which in this case is the KIE, as illustrated in Figure 7 by the Boltzmann distribution using an arbitrarily higher temperature of 500 K.

However, the majority (if not all) of the reactive collisions would have less than optimal orientation and be more likely to get trapped in the reaction complex potential well as the collision

kinetic energy is inefficiently coupled with the reaction coordinate and transferred into the internal degrees of freedom instead. The excess energy in this “hot” complex can certainly re-converge into the association mode and dissociate back to reactants or surmount the barrier to products by re-converting the excess internal energy into potential energy. Collision with the helium buffer gas can occur if the lifetime of such species is long enough, which would increase with the system size and also depend on the characteristics of the PES. If during this competing mechanism enough energy is transferred to the buffer gas to cool the complex below both the reactant and transition-state energy levels, then the complex becomes long lived and can be detected. These collisions would not be reactive and therefore do not contribute to the KIE. Thus, failure to observe the association reaction suggests but does not prove that the reaction proceeds faster (either through the TS to products or back to reactants) than the collision with helium, as found in these reactions.^{30,31} However, the observation of such complexes does not suggest the opposite since assuming that those collisions yielding the complexes are comparable to those yielding product might not be correct in most cases. In principle, one would expect the TST to be valid in such a scenario. Indeed, we find excellent agreement between experimental and theoretical KIE values in these reactions.

On the other extreme, in fast reactions with large negative activation barriers, the rate-limiting step is not the crossing of the transition state but instead the collisional rate (Figure 1). Although one could still try to calculate the KIEs for such reactions using TST, clearly it might not yield meaningful results. In such fast reactions all reacting collisions would have enough energy to surmount both the H' and D' barriers in Figure 7, and the KIE should be close to 1, whereas TST would still predict very inverse KIEs since these calculated values are not dependent on the magnitude or sign of the barrier. Instead, a collisional-controlled reaction would show a KIE that is the ratio of k_{col} for both isotopomers.⁷³ The KIEs calculated this way are normal and close to unity; for instance, the solvent KIE predicted for the reaction of $F^-(H_2O)$ with CH_3I , the fastest reaction in Table 1, is 1.02. This reaction is expected to have a negative activation barrier, as it is even faster than the reaction of $F^-(H_2O)$ with CH_3Br , which already shows a negative barrier^{48,49} (see above). However, it shows an efficiency of only 45%, indicating that more than one-half of the collisions experience a barrier for reaction likely originated by a wrong orientation. This value is consistent with ab initio molecular dynamic simulations, which suggest that less than 50% of the collisions proceed to products in the reaction of $F^-(H_2O)$ with CH_3Cl .^{74,75} Therefore, it is not unlikely that some collisions without an optimal orientation would experience some barrier around the traditional transition-state area.

We interpret our experimental results as a gradual transition between reactions exhibiting a rate-limiting step changing from surmounting the TS to collision rate as the reaction rate increases. As can be seen in Table 1, excellent agreement between experiment and TST is observed for slow reactions. However, reactions that are very efficient and therefore show large negative activation energies display KIEs that are intermediate between the TST and collisional values. It is interesting to note that even for the fastest reaction included in this report, $F^-(H_2O)$ with CH_3I , the observed solvent KIE, 0.89, is still substantially lower than the 1.02 value calculated from collisional rates.

We also looked at other relationships between experimental KIE values. We found that for reactions with low efficiency

the solvent and neutral KIEs seem to be additive, i.e., addition of the experimental KIEs from the solvent and the neutral reactant agrees with the value obtained from the ratio of the perprotio and perdeutero rate constants.^{30,31} Such an agreement is remarkable and predicted by TST. Those reactions with larger efficiency seem to deviate more, and additivity does not hold as well. In other words, estimation of the reaction barrier could be determined in principle by measuring the appropriate KIEs. Unfortunately, deviations from additivity are small in comparison to the error bars in the KIEs, even for the fastest reactions included in this report, and no solid conclusion can be drawn at this point. Measurement of the experimental KIE values with smaller error bars would be required to formulate any clear conclusion, particularly for fast reactions, which incidentally are more difficult to determine experimentally as revealed by the larger error bars shown in these values.^{30,31}

Conclusions

We performed an exhaustive analysis of the origin of the solvent deuterium kinetic isotope effect in the S_N2 reaction mechanism between water, methanol, and HF solvated fluoride anions with methyl halides. We also extended our analysis to the neutral secondary KIEs. We found that in all cases the usually inverse KIE (<1) is due to only a few vibrational modes, in agreement with previous results.^{32,33,39,56} We also found that the product of the rotational, translational, and corresponding low vibrational modes in the transition states correlating with those degrees of freedom in reactants yields a unity or slightly normal contribution to the total isotope effect, in agreement with our previous results for other S_N2 reactions.³³ These modes should be considered together as a group for an adequate KIE analysis. Our results for the solvent KIEs identify the X–H (X = O, F) stretching frequency as the main factor in determining the inverse nature of the solvent KIE since the bond becomes stronger as the reaction proceeds from the reactants to the transition state, in agreement with a previous report on the reaction of monohydrated fluoride ion with methyl chloride.⁵⁶

We have shown that some of the calculated KIEs agree very well with the experimental values, but some do not, and that the disagreement between theory and experiment is related to the reaction efficiency and reaction barrier. We also proposed an explanation for the disagreement in terms of a gradual transition between reactions exhibiting a rate-limiting step that changes from surmounting the TS to a collision-controlled rate as the reaction rate increases and the failure of the TST to model effective barrierless reactions. These fast reactions show experimental values that are consistently closer to unity (less inverse) than the theoretical ones; however, they never reach the slightly normal KIE predicted by their collisional rates. We also stressed the importance of further understanding the dynamics of these reactions.⁷⁴

In addition, isotopic substitution has proven to be a great test for theory as one can make fine adjustments to the barrier, which can be predicted accurately by computational methods, without modifying other reaction conditions including the underlying electronic potential-energy surface, which is much more difficult to predict accurately or determine experimentally.

Acknowledgment. We appreciate the support of this work by the University of Idaho.

Supporting Information Available: Structural information, energies, and vibrational frequencies for all reactants and transition-state isotopomers; table of absolute and relative

energies and free energies. This material is available free of charge via the Internet at <http://pubs.acs.org>.

References and Notes

- (1) March, J. *Advanced Organic Chemistry: Reactions, Mechanisms, and Structure*, 4th ed.; John Wiley & Sons: New York, 1992.
- (2) Shaik, S. S.; Schlegel, H. B.; Wolfe, S. *Theoretical Aspects of Physical Organic Chemistry. The S_N2 Mechanism*; Wiley: New York, 1992.
- (3) Laerdahl, J. K.; Uggerud, E. *Int. J. Mass Spectrom.* **2002**, 214, 277.
- (4) Olmstead, W. N.; Brauman, J. I. *J. Am. Chem. Soc.* **1977**, 99, 4219.
- (5) Chabincyn, M. L.; Craig, S. L.; Regan, C. K.; Brauman, J. I. *Science* **1998**, 279, 1882.
- (6) Wilbur, J. L.; Brauman, J. I. *J. Am. Chem. Soc.* **1991**, 113, 9699.
- (7) DePuy, C. H.; Gronert, S.; Mullin, A.; Bierbaum, V. M. *J. Am. Chem. Soc.* **1990**, 112, 8650.
- (8) Gronert, S.; DePuy, C. H.; Bierbaum, V. M. *J. Am. Chem. Soc.* **1991**, 113, 4009.
- (9) Gonzales, J. M.; Allen, W. D.; Schaefer, H. F., III. *J. Phys. Chem. A* **2005**, 109, 10613.
- (10) Gonzales, J. M.; Pak, C.; Cox, R. S.; Allen, W. D.; Schaefer, H. F., III; Csaszar, A. G.; Tarczay, G. *Chem.—Eur. J.* **2003**, 9, 2173.
- (11) Hase, W. L. *Science* **1994**, 266, 998.
- (12) Jansson, A.; Koskinen, H.; Maentsaelae, P.; Niemi, J.; Schneider, G. *J. Biol. Chem.* **2004**, 279, 41149.
- (13) Iwig, D. F.; Grippe, A. T.; McIntyre, T. A.; Booker, S. J. *Biochemistry* **2004**, 43, 13510.
- (14) Mihel, I.; Knipe, J. O.; Coward, J. K.; Schowen, R. L. *J. Am. Chem. Soc.* **1979**, 101, 4349.
- (15) Gray, C. H.; Coward, J. K.; Schowen, K. B.; Schowen, R. L. *J. Am. Chem. Soc.* **1979**, 101, 4351.
- (16) Hegazi, M. F.; Borchardt, R. T.; Schowen, R. L. *J. Am. Chem. Soc.* **1979**, 101, 4359.
- (17) Rodgers, J.; Femec, D. A.; Schowen, R. L. *J. Am. Chem. Soc.* **1982**, 104, 3263.
- (18) DeTuri, V. F.; Hintz, P. A.; Ervin, K. M. *J. Phys. Chem. A* **1997**, 101, 5969.
- (19) Bohme, D. K.; Mackay, G. I.; Payzant, J. D. *J. Am. Chem. Soc.* **1974**, 96, 4027.
- (20) Tanaka, K.; Mackay, G. I.; Payzant, J. D.; Bohme, D. K. *Can. J. Chem.* **1976**, 54, 1643.
- (21) DePuy, C. H. *Int. J. Mass Spectrom.* **2000**, 200, 79.
- (22) DePuy, C. H. *J. Org. Chem.* **2002**, 67, 2393.
- (23) Regan, C. K.; Craig, S. L.; Brauman, J. I. *Science* **2002**, 295, 2245.
- (24) Takashima, K.; Riveros, J. M. *Mass Spectrom. Rev.* **1998**, 17, 409.
- (25) Bohme, D. K.; Mackay, G. I. *J. Am. Chem. Soc.* **1981**, 103, 978.
- (26) Bohme, D. K.; Raksit, A. B. *J. Am. Chem. Soc.* **1984**, 106, 3447.
- (27) Bohme, D. K.; Raksit, A. B. *Can. J. Chem.* **1985**, 63, 3007.
- (28) Bogdanov, B.; McMahon, T. B. *Int. J. Mass Spectrom.* **2005**, 241, 205.
- (29) Kato, S.; Davico, G. E.; Lee, H. S.; DePuy, C. H.; Bierbaum, V. M. *Int. J. Mass Spectrom.* **2001**, 210, 223.
- (30) Kato, S.; Hacaloglu, J.; Davico, G. E.; DePuy, C. H.; Bierbaum, V. M. *J. Phys. Chem. A* **2004**, 108, 9887.
- (31) O'Hair, R. A. J.; Davico, G. E.; Hacaloglu, J.; Dang, T. T.; DePuy, C. H.; Bierbaum, V. M. *J. Am. Chem. Soc.* **1994**, 116, 3609.
- (32) Davico, G. E. *Org. Lett.* **1999**, 1, 1675.
- (33) Davico, G. E.; Bierbaum, V. M. *J. Am. Chem. Soc.* **2000**, 122, 1740.
- (34) Poirier, R. A.; Wang, Y.; Westaway, K. C. *J. Am. Chem. Soc.* **1994**, 116, 2526.
- (35) Pham, T. V.; Fang, Y.; Westaway, K. C. *J. Am. Chem. Soc.* **1997**, 119, 3670.
- (36) Wolfe, S.; Kim, C. K. *J. Am. Chem. Soc.* **1991**, 113, 8056.
- (37) Boyd, R. J.; Kim, C. K.; Shi, Z.; Weinberg, N.; Wolfe, S. *J. Am. Chem. Soc.* **1993**, 115, 10147.
- (38) Moliner, V.; Williams, I. H. *J. Am. Chem. Soc.* **2000**, 122, 10895.
- (39) Hu, W. P.; Truhlar, D. G. *J. Am. Chem. Soc.* **1995**, 117, 10726.
- (40) Tucker, S. C.; Truhlar, D. G. *J. Phys. Chem.* **1989**, 93, 8138.
- (41) Tucker, S. C.; Truhlar, D. G. *J. Am. Chem. Soc.* **1990**, 112, 3338.
- (42) Zhao, X. G.; Lu, D. H.; Liu, Y. P.; Lynch, G. C.; Truhlar, D. G. *J. Chem. Phys.* **1992**, 97, 6369.
- (43) Glad, S. S.; Jensen, F. *J. Am. Chem. Soc.* **1997**, 119, 227.
- (44) Hasanayn, F.; Streitwieser, A.; Al-Rifai, R. *J. Am. Chem. Soc.* **2005**, 127, 2249.
- (45) Rodgers, J.; Femec, D. A.; Schowen, R. L. *J. Am. Chem. Soc.* **1982**, 104, 3263.
- (46) Viggiano, A. A.; Paschkewitz, J.; Morris, R. A.; Paulson, J. F.; Gonzalez-Lafont, A.; Truhlar, D. G. *J. Am. Chem. Soc.* **1991**, 113, 9404.
- (47) Zhao, X. G.; Tucker, S. C.; Truhlar, D. G. *J. Am. Chem. Soc.* **1991**, 113, 826.

- (48) Viggiano, A. A.; Arnold, S. T.; Morris, R. A. *Int. Rev. Phys. Chem.* **1998**, *17*, 147.
- (49) Seeley, J. V.; Morris, R. A.; Viggiano, A. A. *J. Phys. Chem. A* **1997**, *101*, 4598.
- (50) Seeley, J. V.; Morris, R. A.; Viggiano, A. A.; Wang, H. B.; Hase, W. L. *J. Am. Chem. Soc.* **1997**, *119*, 577.
- (51) Viggiano, A. A.; Arnold, S. T.; Morris, R. A.; Ahrens, A. F.; Hierl, P. M. *J. Phys. Chem.* **1996**, *100*, 14397.
- (52) Okuno, Y. *Chem. Phys. Lett.* **1997**, *264*, 120.
- (53) Swain, C. G.; Bader, R. F. W. *Tetrahedron* **1960**, *10*, 182.
- (54) Buntoa, C. A.; Shiner, V. J., Jr. *J. Am. Chem. Soc.* **1961**, *83*, 3207.
- (55) Bunton, C. A.; Shiner, V. J., Jr. *J. Am. Chem. Soc.* **1961**, *83*, 42.
- (56) Hu, W.-P.; Truhlar, D. G. *J. Am. Chem. Soc.* **1994**, *116*, 7797.
- (57) Frisch, M. J.; Trucks, G. W.; Schlegel, H. B.; Scuseria, G. E.; Robb, M. A.; Cheeseman, J. R.; Zakrzewski, V. G.; Montgomery, J. A.; Stratmann, R. E.; Burant, J. C.; Dapprich, S.; Millam, J. M.; Daniels, A. D.; Kudin, K. N.; Strain, M. C.; Farkas, O.; Tomasi, J.; Barone, V.; Cossi, M.; Cammi, R.; Mennucci, B.; Pomelli, C.; Adamo, C.; Clifford, S.; Ochterski, J.; Petersson, G. A.; Ayala, P. Y.; Cui, Q.; Morokuma, K.; Malick, D. K.; Rabuck, A. D.; Raghavachari, K.; Foresman, J. V.; Cioslowski, J.; Ortiz, J. V.; Baboul, A. G.; Stefanov, B. B.; Liu, G.; Liashenko, A.; Piskorz, P.; Komaromi, I.; Gomperts, R.; Martin, R. L.; Fox, D. J.; Keith, T.; Al-Laham, M. A.; Peng, C. Y.; Nanayakkara, A.; Gonzales, C.; Challacombe, M.; Gill, P. M. W.; Johnson, B.; Chen, W.; Wong, M. W.; Andres, J. L.; Head-Gordon, M.; Replogle, E. S.; Pople, J. A. *Gaussian 98*, Revision A.9; Gaussian, Inc.: Pittsburgh, PA, 1998.
- (58) Hay, P. J.; Wadt, W. R. *J. Chem. Phys.* **1985**, *82*, 270.
- (59) Wadt, W. R.; Hay, P. J. *J. Chem. Phys.* **1985**, *82*, 284.
- (60) Hay, P. J.; Wadt, W. R. *J. Chem. Phys.* **1985**, *82*, 299.
- (61) Glukhovtsev, M. N.; Pross, A.; Radom, L. *J. Am. Chem. Soc.* **1995**, *117*, 2024.
- (62) Schwartz, R. L.; Davico, G. E.; Ramond, T. M.; Lineberger, W. C. *J. Phys. Chem. A* **1999**, *103*, 8213.
- (63) Davico, G. E. *J. Phys. Chem. A* **2005**, *109*, 3433.
- (64) Dunning, T. H., Jr. *J. Chem. Phys.* **1989**, *90*, 1007.
- (65) Woon, D. E.; Dunning, T. H., Jr. *J. Chem. Phys.* **1993**, *98*, 1358.
- (66) Eyring, H. *J. Chem. Phys.* **1935**, *3*, 107.
- (67) Gonzalez-Lafont, A.; Truong, T. N.; Truhlar, D. G. *J. Phys. Chem.* **1991**, *95*, 4618.
- (68) Combariza, J. E.; Kestner, N. R. *J. Phys. Chem.* **1994**, *98*, 3513.
- (69) Okuno, Y. *J. Am. Chem. Soc.* **2000**, *122*, 2925.
- (70) Adamovic, I.; Gordon, M. S. *J. Phys. Chem. A* **2005**, *109*, 1629.
- (71) Glukhovtsev, M. N.; Bach, R. D.; Pross, A.; Radom, L. *Chem. Phys. Lett.* **1996**, *260*, 558.
- (72) Parthiban, S.; de Oliveira, G.; Martin, J. M. L. *J. Phys. Chem. A* **2001**, *105*, 895.
- (73) Su, T.; Chesnavich, W. J. *J. Chem. Phys.* **1982**, *76*, 5183.
- (74) Tachikawa, H. *J. Phys. Chem. A* **2000**, *104*, 497.
- (75) Tachikawa, H. *J. Phys. Chem. A* **2001**, *105*, 1260.